ISSN 2580-0817


# Numerical Analysis of the Effect of Vortex Generator on the Aerodynamic Performance of NACA 6412 Airfoils Using Large Eddy Simulation

Dedet Hermawan Setiabudi[1], Joan Bayuaji Nugroho[1*], Eli Kumolosari[1], Lazuardy Rahendra Pinandhita[2], Okto Dinaryanto[1]

[1]*Mechanical Engineering, Adisutjipto Institute of Aerospace Technology, Jl. Janti / Jl. Majapahit Blok-R Yogyakarta 55198, Indonesia*
[2]*Aerospace Engineering, Adisutjipto Institute of Aerospace Technology, Jl. Janti / Jl. Majapahit Blok-R Yogyakarta 55198, Indonesia*
**Corresponding author: nugrohojoanbayuaji@gmail.com*

*Article history:*
Received: 1 August 2025 / Received in revised form: 6 October 2025 / Accepted: 12 October 2025
Available online 30 October 2025

ABSTRACT

Aerodynamic performance of an airfoil is significantly affected by flow separation, especially at high angles of attack. One common strategy to control flow separation is adding a triangular vortex generator (VG), which creates small vortices that help keep the airflow attached. The present study investigated the impact of triangular vortex generators on a NACA 6412 airfoil using Computational Fluid Dynamics (CFD) method. Large Eddy Simulation (LES) was applied due to its ability to show the vortices more clearly than other methods. It can also accurately capture the flow separation. To obtain the lift, drag, and lift-to-drag ratio ($C_L/C_D$) data, four angles of attack (0°, 5°, 10°, and 15°) and four velocities (10, 15, 20, and 25 m/s) were examined. The results indicate that at low AoA, VG increases drag and decreases aerodynamic efficiency. VG, on the other hand, makes flow attachment better, delays separation, and narrows the wake region at medium to high angles of attack. The most improvement in $C_L/C_D$, up to 83%, occurred at AoA of 15°. These results show that adding triangular VG can improve aerodynamic efficiency in critical situations close to stall and lay the groundwork for creating more advanced flow-control systems in more complicated aerodynamic situations.



***Keywords:*** *Aerodynamic performance, CFD, large Eddy simulation, vortex generator.*

## I. Introduction

Aerodynamic performance is an important part of designing and running aviation systems because it affects flight safety, stability, and efficiency directly [1]. Research and development in the aerospace field have moved quickly since Horatio F. Phillips found the chambered profile in 1884 and the Wright brothers flew their first aeroplane in 1903 [2].

The flow separation phenomenon is one of the biggest problems in aerodynamics, especially when the angle of attack (AoA) is high and the velocity is low [3]. Flow separation occurs when the airflow starts to move away from the surface of the aerofoil because the flow momentum can't overcome the shear stress and pressure gradient. If this happens more often, it could cause a stall, which could put flight operations at risk [4]. Because of this, it has become very important to come up with ways to control airflow so that it stays attached to the surface. This is especially true to delay flow separation and make the aerofoil work better aerodynamically.

DOI: 10.17977/um016v9i2p479

Various approaches have been investigated to overcome this flow separation, which are generally divided into two categories: active control and passive control [5]. Vortex generators (VGs) are an example of a passive control method that is commonly used, not only in aircraft, but has also been developed to overcome flow separation in wind turbines [6]. Vortex generators are widely used due to their cost-effectiveness, simplicity, and ease of implementation under various conditions [7]. The vortex generator functions by creating an air vortex on the surface of the airfoil. This vortex possesses higher momentum, which adds energy to the boundary layer and ultimately helps delay flow separation [8]. Several studies have demonstrated that the geometric shape of the VG, its placement location, and dimensions have a significant impact on its effectiveness in enhancing the lift coefficient and improving the aerodynamic value ($C_L/C_D$ ratio) [9]. Dharmawan *et al.* modified the Eppler 562 airfoil using a Gothic-shaped VG with a counter-rotating configuration. The results showed that the airfoil with the Gothic VG was more stable, as evidenced by the visualization that the VG could slow down the flow separation and prevent the formation of a turbulent boundary layer, thus increasing its aerodynamic performance [10].

Although various studies have been conducted on symmetric airfoils using vortex generators, similar studies on asymmetrical airfoils, such as the NACA 6412, are still very limited [11-14]. In fact, asymmetrical airfoils are widely applied in Unmanned Aerial Vehicles (UAVs), gliders, and even in applications like wind turbines. This is because this type of airfoil generates high lift even at low angles of attack [15]. Furthermore, most previous studies have used the RANS (Reynolds-Averaged Navier-Stokes) approach, which is unable to capture the vortex and turbulence transition phenomena in detail. Therefore, a numerical study using the large Eddy simulation (LES) method is needed to analyze the flow behavior around the VG in more detail. To date, no study has specifically examined triangular vortex generators on the NACA 6412 airfoil using LES, underscoring the novelty and importance of this research [16-18]. Indeed, the LES method provides a more accurate and detailed depiction of the airflow behavior around vortex generators than conventional approaches like RANS [19-21]. Therefore, a quantitative study on the comparison of the aerodynamic performance of the NACA 6412 airfoil with and without VG, especially using the LES approach, is needed to provide accurate data on the phenomena in aerodynamics.

This study specifically aimed to evaluate the impact of the use of a triangular vortex generator on the aerodynamic characteristics of the NACA 6412 airfoil through CFD simulations using the LES method. CFD (Computational Fluid Dynamics) is a widely used method that is applicable for modelling various phenomena. The main focus of this study included the analysis of changes in lift, drag, and aerodynamic efficiency ($C_L/C_D$), in addition to exploring flow behavior such as streamline patterns and velocity contour distributions due to the installation of the vortex generator. In addition, this study examined the effect of variations in flow velocity and angle of attack, intending to obtain a comprehensive understanding of the performance of the vortex generator under various operational conditions. Thus, the results of this study not only provide a fundamental understanding of the flow characteristics around the VG, but can also be used as a practical design reference in aerodynamic engineering for the aerospace sector, renewable energy, and the development of unmanned vehicle technology.

## II. Material and Methods

### *1. Method*

This study was conducted to determine the effect of a triangular vortex generator on the aerodynamic characteristics of the NACA 6412 airfoil using CFD. The viscous model applied was the LES. This viscous model was chosen because it can model turbulent flow with high accuracy, especially in detecting the formation and movement of vortices around the boundary layer [22].

Figure 1 shows the main stages in the research process. It begins with a literature review, followed by determining an appropriate mathematical model. This is followed by creating a baseline airfoil and then starting the simulation setup. The results of this first simulation are used for validation testing between the simulation results and the Xfoil database. If the error reaches <20%, it can be concluded that the parameters are appropriate and can proceed to the airfoil modification stage by adding a triangular vortex generator, which concludes with data collection, analysis, and discussion.

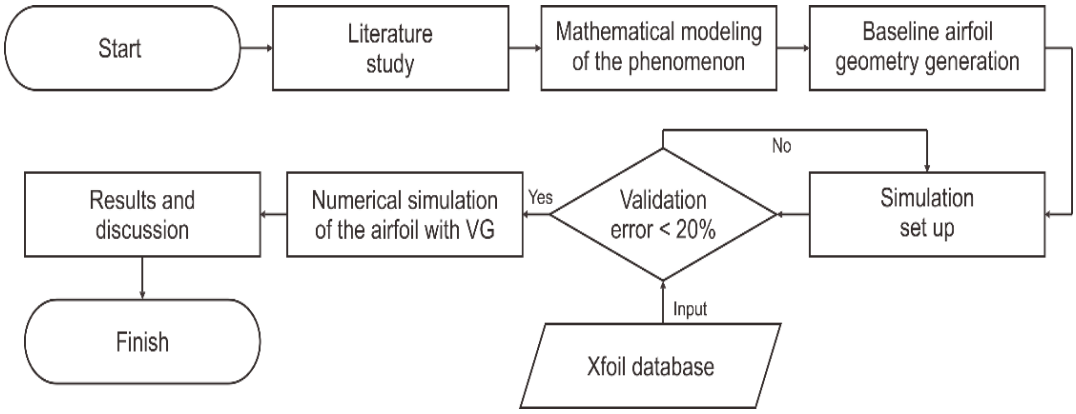


Fig. 1. Research Flowchart

### *2. Design and Material*

This study was conducted using Ansys Student 2024 R2 software. The geometry of the NACA 6412 airfoil was modeled in two configurations: the baseline airfoil and the airfoil with VG addition. The geometry model is shown in Figures 2 (a and b), while the domain is shown in Figure 3 and the meshing results is shown in Figures 4 and 5.

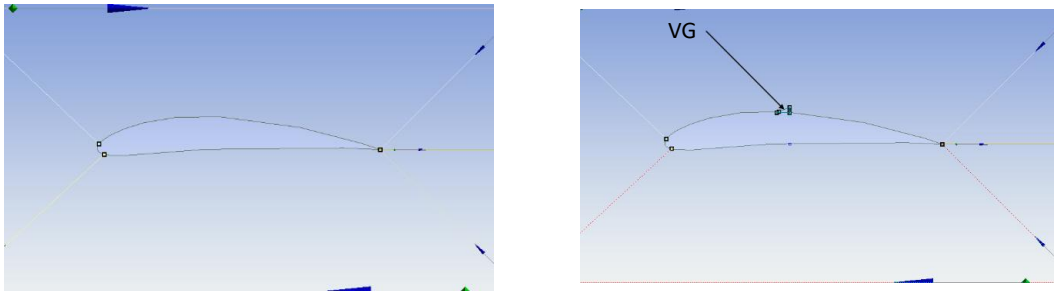


Fig. 2. Baseline airfoil (a) vs VG airfoil (b)

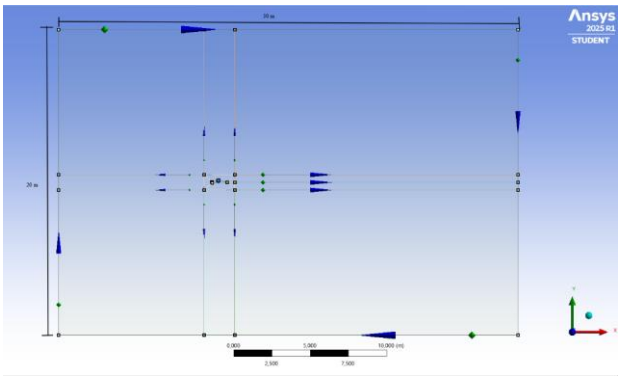


Fig. 3. Simulation domain

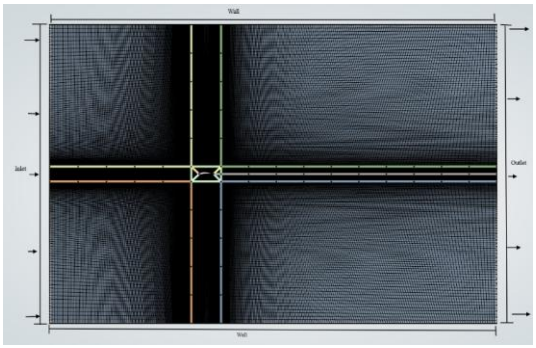

Fig. 4. Meshing result

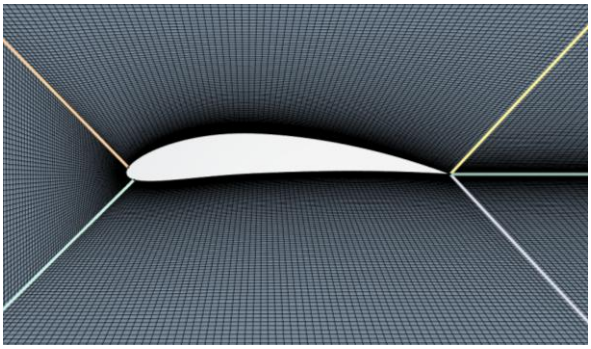

Fig. 5. Inflation meshing

## 3. *Set-up*

The simulation setup was performed in the Ansys software with transient flow using the LES approach. LES was chosen due to its ability to represent vortex flow better [23]. Although it also has some weaknesses, one of them is the longer computational time needed. The subground-scale model chosen was WALE (Wall-Adapting Local Eddy-viscosity), which is designed to provide accurate predictions of flow near walls [24]. The general parametric setup is shown in Table 1.

**Table 1.** Simulation parameter

| Parameter | Description |
|---|---|
| Airfoil type | NACA 6412 |
| Chord length | 1 m |
| Vortex generator type | Triangular, length 4% C & height 2% C |
| VG location | 45% C |
| Solver | Pressure-based, transient |
| Turbulence model | LES |
| Subgrid–scale model | WALE |
| Momentum | Second order upwind |
| Coupling | Simple |
| AOA | 0°, 5°, 10°, 15° |
| Density | 1.164 kg/m$^3$ |
| Viscosity | 1.872 x 10$^{-5}$ Kg/m.s |
| Temperature conditions | 303.15 K |
| Pressure conditions | 102500 Pascal |
| Velocity | 10, 15, 20, 25 m/s |

This research generally used the principles of conservation of mass and conservation of momentum (Navier–Stokes), expressed in Eq. (1) and Eq. (2).

$$\frac{\partial(\rho)}{\partial t} + \nabla.(\rho \boldsymbol{u}) = 0 \quad \text{..... (1)}$$

$$\frac{\partial}{\partial t}(\rho \boldsymbol{u}) + \nabla.(\rho \boldsymbol{u}.\boldsymbol{u}) = -\nabla p + \nabla.[\mu(\nabla \boldsymbol{u} + \nabla \boldsymbol{u}^T)] + \rho \boldsymbol{g} + \boldsymbol{F} \text{..... (2)}$$

The lift and drag coefficients can be calculated using Eq. (3) and Eq. (4).

$$C_L = \frac{L}{\frac{1}{2}\rho V^2 S} \quad \text{..... (3)}$$

$$C_D = \frac{D}{\frac{1}{2}\rho V^2 S} \quad \text{..... (4)}$$

Where: L = Lift; P = Air density; V = Aircraft velocity; S = Wing surface area; $C_L$ = Lift coefficient; $C_D$ = Drag coefficient

## III. Results and Discussions

### *1. Validation*

The results of the simulation were used in a validation study to ensure the appropriate parameters were used. Due to the limitations of the previous experimental study on NACA 6412, validation was performed by comparing the simulation results with predictions from the Xfoil database. The results of the validation study are presented in Table 2.

**Table 2.** The results of the validation study

| Vel | AoA | Reynolds Number | CFD | | | XFOIL | | | Error (%) | | |
|---|---|---|---|---|---|---|---|---|---|---|---|
| | | | $C_L$ | $C_D$ | $C_L/C_D$ | $C_L$ | $C_D$ | $C_L/C_D$ | $C_L$ | $C_D$ | $C_L/C_D$ |
| 19 | 8 | 1 x $10^6$ | 1.2626 | 0.01011 | 124.9 | 1.4931 | 0.01135 | 131.6 | 15.4 | 10.9 | 5.1 |
| 19 | 10 | 1 x $10^6$ | 1.2418 | 0.01428 | 86.98 | 1.5846 | 0.01815 | 87.28 | 21.6 | 21.3 | 0.37 |

Table 2 shows that the error percentages for $C_L$, $C_D$, and $C_L/C_D$ values are <20%. This indicates that the simulation parameters were appropriate and can proceed to the mesh independence test stage.

### *2. Mesh Independence Test*

Although the present study employed a 2D approach for NACA 6412, the setup was designed to obtain as accurate data as possible. One of the efforts was the grid independence study. This aims to ensure that simulation results are not affected by the mesh size and density used. In CFD-based simulations, using meshes that are too coarse will produce inaccurate data, while meshes that are too fine will require longer computational time. Therefore, several simulations were conducted with varying numbers of elements to observe changes in $C_L$ and $C_D$ values. If the simulation results show no significant difference between two or more meshes, it can be concluded that the meshing has reached an ideal condition. Increasing the number of elements will only increase computational time and weight, but the results achieved will not differ significantly. This aims to obtain accurate simulation results while remaining efficient in terms of time and resources.

In the grid independence test, the study begins with the largest mesh. It then successively reduces it to achieve the most efficient results without sacrificing the details of the simulation results. In the grid independence study, Eq. (5) is used.

$$Error = \frac{X_i - X_{i-1}}{X_i} 100\% \quad (5)$$

Where $X_i$ : CFD value;

$X_{i-1}$ : Xfoil reference value

By this formula, the results of the grid independence test study are obtained in Table 3.

**Table 3.** Mesh independence test

| No. | Velo-city | AoA | Number of Nodes | Number of Elements | CFD | | | Error % | | |
|---|---|---|---|---|---|---|---|---|---|---|
| | | | | | $C_L$ | $C_D$ | $C_L/C_D$ | $C_L$ | $C_D$ | $C_L/C_D$ |
| 1. | 19 | 8 | 14229 | 13836 | 0.5612 | 0.0943 | 5.95 | 62.4 | 730.6 | 95.5 |
| 2. | 19 | 8 | 29917 | 29413 | 0.7965 | 0.08879 | 8.97 | 46.6 | 682 | 93.2 |
| 3. | 19 | 8 | 64461 | 63767 | 0.9312 | 0.07153 | 13.01 | 37.6 | 529.9 | 90.1 |
| 4. | 19 | 8 | 114017 | 112381 | 1.3241 | 0.0517 | 25.61 | 11.3 | 544.3 | 80.5 |
| 5. | 19 | 8 | 207953 | 206769 | 1.2626 | 0.01011 | 124.9 | 15.4 | 10.9 | 5.1 |
| 6. | 19 | 8 | 330263 | 327997 | 1.3747 | 0.01152 | 119.3 | 7.95 | 0.26 | 9.3 |

The table indicates that a finer mesh generally results in a smaller relative error. However, in the sixth mesh configuration, although the errors in $C_L$ and $C_D$ compared to Xfoil are slightly smaller, the percentage error in the $C_L/C_D$ ratio increases to 9.3%, higher than the lowest value observed in the fifth mesh. In the context of aerodynamic efficiency, a lower percentage error in the $C_L/C_D$ ratio indicates better performance, as it reflects a higher lift with lower drag.

Therefore, the 5th mesh (207,953 nodes) was chosen as the optimum mesh, as it produced the highest $C_L/C_D$ value with the lowest error. The addition of elements to the 6th mesh did not provide any performance improvement, but instead decreased aerodynamic efficiency and significantly increased computational time. Thus, the simulation results on the 5th mesh have met the numerical convergence requirements with sufficient computational efficiency, so they can be used in the next stage.

## *3. Result*

Table 4 presents the research results, including the coefficient of lift and drag values. The lift and drag coefficient calculations are obtained from the lift and drag force calculations generated by simulations using the LES method. This method generates fluctuating simulation data that represent the true nature of turbulent flow. Therefore, this method requires a longer computational time, especially when applied to a 3D approach.

**Table 4.** Aerodynamics parameters obtained from CFD simulation

| AoA/ Velocity | Baseline Airfoil | | | VG Airfoil | | | Difference | | |
|---|---|---|---|---|---|---|---|---|---|
| | $C_L$ | $C_D$ | $C_L/C_D$ | $C_L$ | $C_D$ | $C_L/C_D$ | $C_L$ | $C_D$ | $C_L/C_D$ |
| **0** | | | | | | | | | |
| 10 | 0.3015 | 0.02183 | 13.81 | 0.48054 | 0.05063 | 9.4912 | +59.4 | +132 | −31.3 |
| 15 | 0.37949 | 0.03026 | 12.541 | 0.50071 | 0.04858 | 10.099 | +31.96 | +60.5 | −19.4 |
| 20 | 0.41952 | 0.03112 | 13.481 | 0.63264 | 0.05186 | 12.199 | +50.80 | +66.7 | −9.5 |
| 25 | 0.54603 | 0.02095 | 26.064 | 0.86819 | 0.04116 | 21.093 | +59.0 | +96.4 | −19.1 |
| **5** | | | | | | | | | |
| 10 | 0.806574 | 0.04255 | 18.956 | 1.09826 | 0.05489 | 19.9821 | +36.2 | +29.0 | +5.4 |
| 15 | 0.862819 | 0.043639 | 19.772 | 1.14682 | 0.05511 | 20.8097 | +32.9 | +26.3 | +5.3 |
| 20 | 1.088561 | 0.051859 | 20.990 | 1.19771 | 0.05601 | 21.3837 | +10.0 | +8.0 | +1.9 |
| 25 | 1.116384 | 0.052431 | 21.292 | 1.240734 | 0.05731 | 21.6490 | +11.1 | +9.3 | +1.7 |
| **10** | | | | | | | | | |
| 10 | 1.297725 | 0.08531 | 15.212 | 1.443235 | 0.07517 | 19.1997 | +11.2 | -11.9 | +26.3 |
| 15 | 1.475231 | 0.12530 | 11.782 | 1.612736 | 0.07941 | 20.3121 | +9.3 | –36.6 | +72.4 |
| 20 | 1.565810 | 0.12348 | 12.688 | 1.681438 | 0.08315 | 20.2143 | +7.4 | –32.6 | +59.4 |
| 25 | 1.58998 | 0.09945 | 15.988 | 1.651560 | 0.09095 | 18.1589 | +3.9 | –8.6 | +13.6 |
| **15** | | | | | | | | | |
| 10 | 1.776378 | 0.31661 | 5.6106 | 1.873922 | 0.17614 | 10.6388 | +5.49 | – 44.37 | +89.63 |
| 15 | 1.919980 | 0.31883 | 6.0334 | 1.945738 | 0.17621 | 11.0421 | +1.34 | – 44.73 | +83.02 |
| 20 | 1.951187 | 0.31023 | 6.2895 | 1.985486 | 0.17522 | 11.3313 | +1.76 | – 43.52 | +80.16 |
| 25 | 2.236472 | 0.32996 | 6.7782 | 2.451838 | 0.21469 | 11.4203 | +9.63 | –34.93 | +68.49 |

The data in Table 4 is also processed in graphic form, which aims to make it easier to represent the influence of VG on the performance of the NACA 6412 airfoil. The graph from Table 4 is depicted in Figure 6.

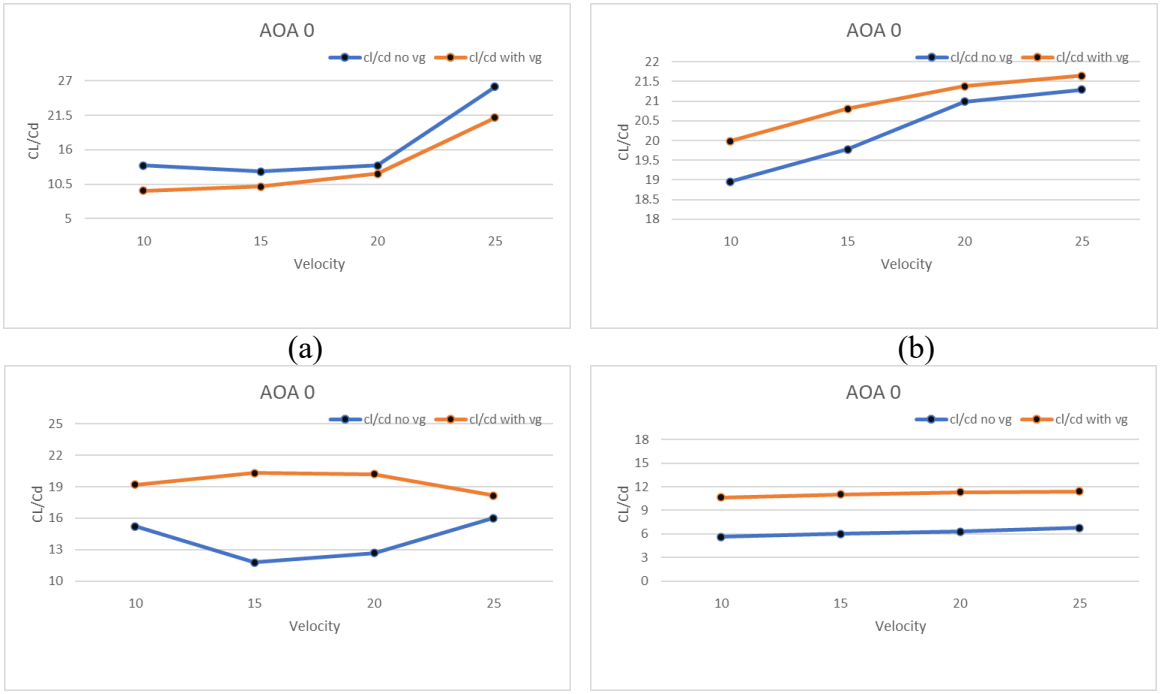


Fig. 6. Graph of $C_L/C_D$ ratio vs velocity at AoA (a) 0º, (b) 5º, (c) 10º and (d) 15º

After quantitative data in the form of aerodynamic coefficient values and representative graphs, the analysis continues with flow visualization through streamlines and velocity contours. Streamlines provide a visual representation of the flow that occurs at each angle of attack and velocity variation, and support the interpretation of the effect of the vortex generator on the reattachment phenomenon after flow separation occurs. The results of the streamline contours are shown in Tables 5-8.

**Table 5.** Streamline contour at AoA 0º for different inlet velocities (10–25 m/s) comparing cases without and with VG

| Velocity (m/s) | AoA 0º | |
|---|---|---|
| | Non VG | With VG |
| 10 | 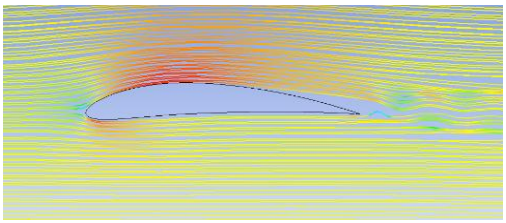 | 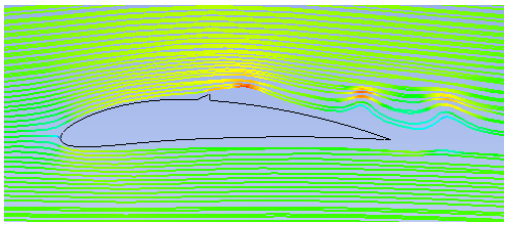 |
| 15 | 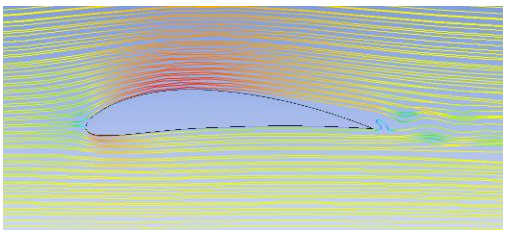 | 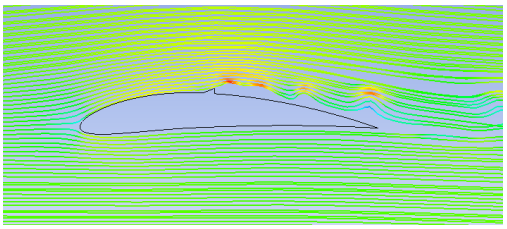 |
| 20 | 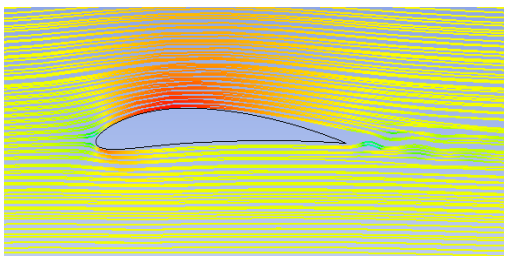 | 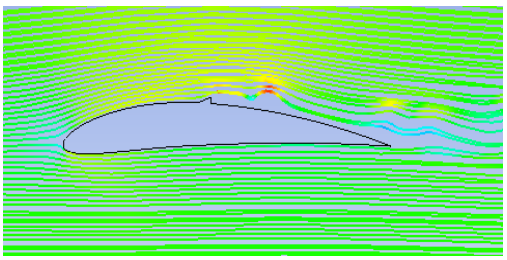 |
| 25 | 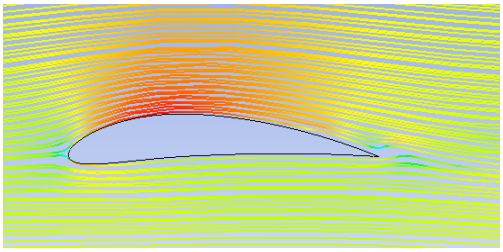 | 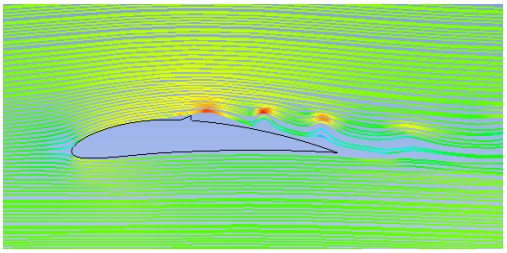 |

At an angle of attack of 0º the boundary layer on the airfoil still tends to be laminar following the contour of the airfoil; the installation of the Vortex generator makes turbulence occur earlier. At a velocity of 10 m/s, there is an addition of $C_L$ by 59.4% accompanied by an addition of $C_D$ by 132% this causes the ratio between $C_L/C_D$ of the airfoil that uses the addition of VG to decrease when compared to the Baseline airfoil. The decrease in the ratio between $C_L/C_D$, which reaches 31.3% indicates that there is an increased drag gradient due to skin friction between the laminar flow and the vortex generator. At a velocity of 15 m/s, the difference in $C_L$ and $C_D$ values decreases when compared to a velocity of 10 m/s, with values of 31.9% and 60.5% respectively. This

causes a decrease in the difference in the $C_L/C_D$ ratio to 19.4%. The downward trend in the $C_L/C_D$ ratio difference continues at a velocity of 20 m/s, where at this velocity the difference in $C_L$ and $C_D$ values increases to 50.8% and 66.7%, resulting in a $C_L/C_D$ value of 9.5%. This indicates that as the velocity increases, the $C_L$ value will increase, resulting in a decrease in the $C_L/C_D$ ratio resulting in a decrease in the efficiency of VG use. An exception is the 25 m/s velocity, where there is a significant increase in $C_L$ and $C_D$ values because at this velocity, the flow has a large kinetic energy and Reynolds Number. Therefore, the efficiency of VG use also increases slightly compared to the 15 m/s and 20 m/s velocities, with a $C_L/C_D$ difference of 19.1%.

Figure 6(a) illustrates that adding a vortex generator at 0° AoA tends to reduce the airfoil's aerodynamic performance compared to the baseline. This aligns with reported findings, which state that at low AoA—when $C_L$ is still low—VGs primarily increase parasitic drag, intensifying the adverse pressure gradient and thus reducing aerodynamic efficiency, though not causing stall [25-26].

**Table 6.** Streamline contours at AoA 5º for different inlet velocities (10–25 m/s) comparing cases without and with VG

| | AoA 5º |
|---|---|
| 10 | 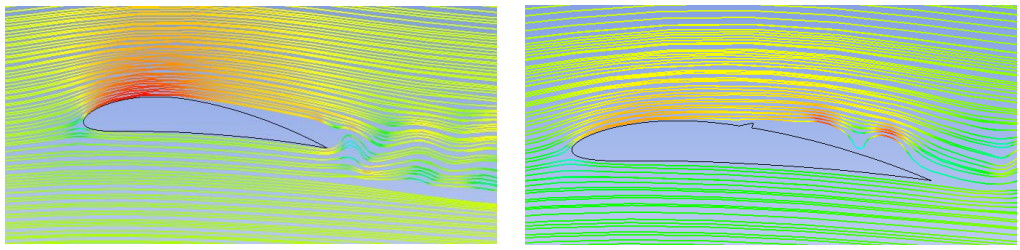 |
| 15 | 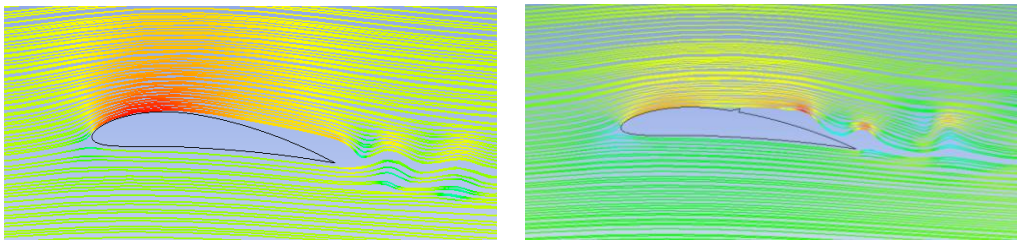 |
| 20 | 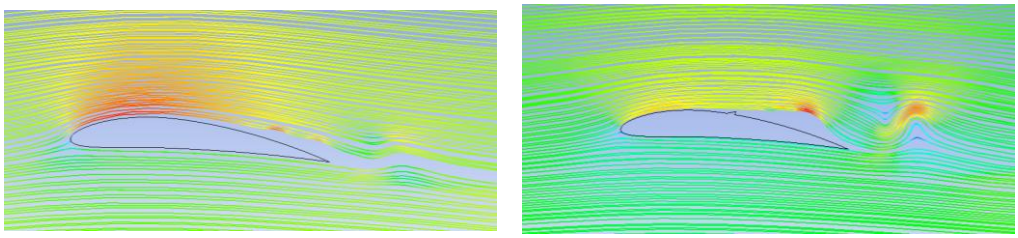 |
| 25 | 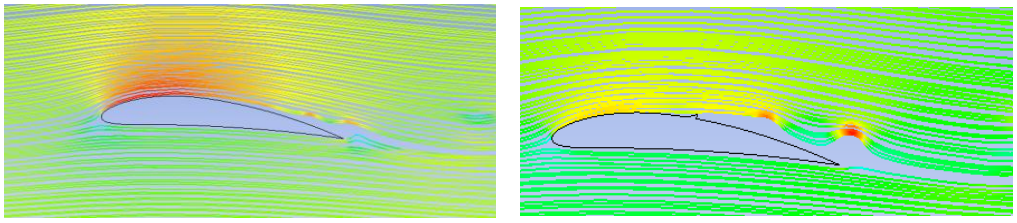 |

The presence of a VG tends to make the $C_L/C_D$ ratio increase in a more linear trend. This indicates that although the vortex generator reduces aerodynamic performance at an

AoA of 0°, it contributes to a more stable coefficient value with minimal fluctuations. Flow visualization with velocity streamline contours (Tables 5-8) shows a pattern consistent with the baseline airfoil, where the airflow remains laminar, closely following the airfoil's contour, indicating that the aerodynamics are functioning as expected. However, when there is an addition of a VG to the airfoil, the airflow becomes chaotic so that the airflow does not adhere perfectly to the boundary layer of the airfoil. This causes a decrease in the aerodynamic performance of the airfoil because the VG only adds skin friction without providing significant benefits.

At an angle of attack of 5º, the airflow begins to differ, especially on the trailing edge, due to the influence of the back pressure gradient on the airfoil surface. In this condition, the use of a VG has an effect on stabilizing the airflow to the airfoil surface. At a velocity of 10 m/s, the addition of a VG results in a significant increase in $C_L$ reaching 36.2% accompanied by an increase in $C_D$ of 29%. Although the values both increase but the increase in $C_L$ is more dominant, so that the ratio between $C_L/C_D$ also increases by around 5.4%. This shows that the Vortex generator is quite effective in increasing the $C_L$ value by encouraging the flow to remain attached to the airfoil surface. At a velocity of 15 m/s, the increase in $C_L$ remains the same with an increase ratio of 32.9% accompanied by an increase in $C_D$ of 26.3% slightly lower when compared to a velocity of 10 m/s. This is understandable because, basically, the simulation pattern using LES results tends to fluctuate. However, the increase in the $C_L/C_D$ ratio at a velocity of 15 indicates that the Vortex generator remains effective in increasing aerodynamic performance at an AoA of 5º. At velocities of 20 m/s and 25 m/s, the effectiveness of the VG begins to decline, with an increase in $C_L$ at 20 m/s of about 10% and an increase in $C_D$ of 8%, resulting in a ratio increase of only about 1.9%. This is reasonable, as higher velocities result in increased kinetic energy and momentum, enabling the flow to overcome adverse pressure gradients more effectively, even without significant contribution from the VG [27]. A similar trend is observed at 25 m/s, where $C_L$ increases by 11.1% and $C_D$ by 9.3%, with a ratio of only 1.7%. Although there is an improvement in performance, the increase is relatively minor. Both of these factors indicate that at higher velocity, the airflow has sufficient momentum to resist separation.

Figure 6(b) shows how the increase in the $C_L/C_D$ ratio due to the use of an effective VG at velocities of 10-15 m/s is indicated by the graph line between the baseline airfoil and the VG airfoil at this velocity, having the largest distance. However, starting from velocities of 20 m/s to 25 m/s, the difference between the two becomes smaller. Visualization of the streamline contour (Tables 5-8) also represents how the airflow on the baseline airfoil looks chaotic at around 60% chord. The addition of a VG induces the vortices that help guide the airflow back toward the airfoil surface, thereby enhancing boundary layer attachment. This vortex flow intensity is shown at velocities of 10-15 m/s and gradually decreases at velocities of 20-25 m/s.

At an angle of attack of 10º, the vortex flow begins to appear larger due to the influence of a stronger adverse pressure gradient on the upper surface of the airfoil. This condition makes the effect of the VG increasingly important. At a velocity of 10 m/s, the VG has a significant effect on the value of lift and drag. The increase in $C_L$ reaches 11.2% while $C_D$ decreases by 11.9%. This increase in $C_L$ and decrease in $C_D$ causes the $C_L/C_D$ ratio to increase by 26.3%. This decrease indicates that VG also reduces drag. When the velocity increases to 15 m/s, the presence of the vortex generator results in an increase in $C_L$ of 9.3% accompanied by a significant decrease in $C_D$, reaching 36.6% resulting in a significant increase in the $C_L/C_D$ ratio of up to 72%. This indicates that the vortex

generator works quite well at medium velocites. It produces a stable flow and maintains attached flow on the airfoil surface. The same thing applies at a velocity of 20 m/s, where $C_L$ increases by 7.4% and $C_D$ decreases by 32.6% with a $C_L/C_D$ ratio increasing by 59.4% proving that the use of a vortex generator forms a vortex flow that makes the flow more controlled and prevents backflow, which makes the drag coefficient increase. At high velocities such as 25 m/s. The vortex generator still provides benefits with an increase in $C_L$ of 3.9% with a decrease in drag of 8.6% with an increase ratio for the $C_L/C_D$ ratio of 13.6%. Although this increase is not as large as before, this makes sense because with a large momentum gradient, the flow is still strong enough to provide lift even without the addition of a vortex generator. This coefficient increase does not appear to increase linearly and tends to be random; this is understandable because basically the simulation using LES is fluctuating following real aerodynamic conditions.

**Table 7.** Streamline contours at AoA 10° for different inlet velocities (10–25 m/s) comparing cases without and with VG

| | AoA 10° | |
|---|---|---|
| 10 | 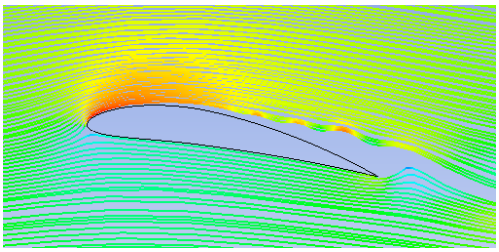 | 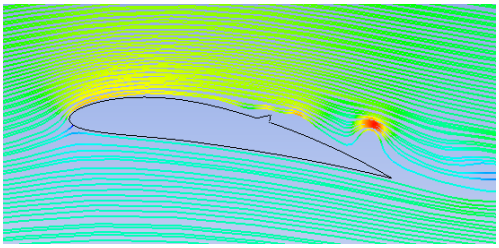 |
| 15 | 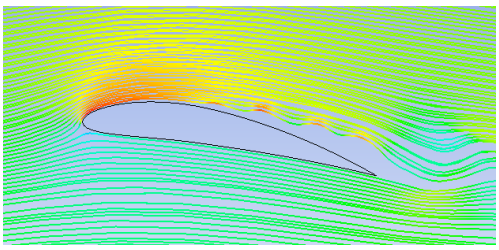 | 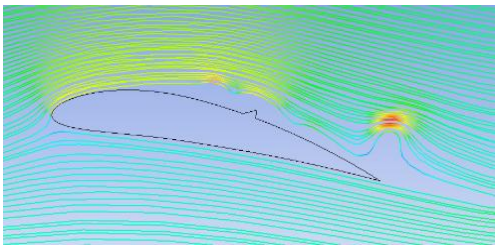 |
| 20 | 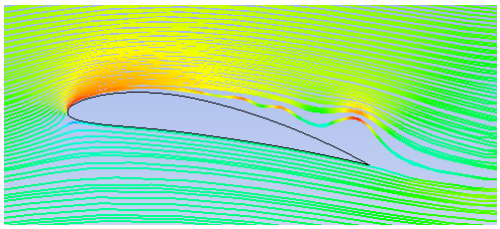 | 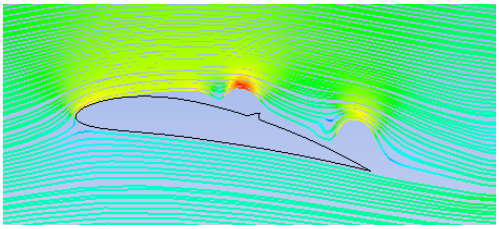 |
| 25 | 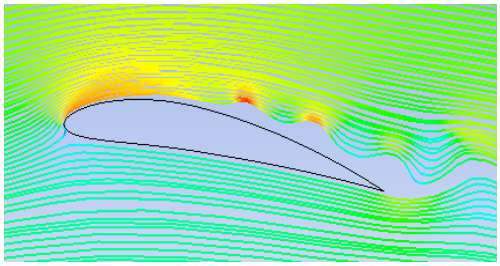 | 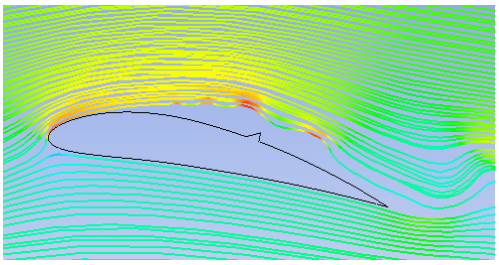 |

The graphical representation (Figure 6) shows how the most significant increase in the $C_L/C_D$ ratio occurs at velocities of 15 and 20 m/s, with a visible gap that is quite large

between the baseline airfoil line and the VG airfoil. This confirms how the VG is effective at medium velocities. The streamline visualization (Tables 5-8) shows how the baseline airfoil experiences flow separation starting from 50% chord from the leading edge. This effect is most pronounced at lower flow velocities (10–15 m/s), where the momentum is insufficient to sustain boundary layer attachment on the airfoil surface. The addition of a VG makes the airfoil flow stick together again because the vortex flow has higher momentum, thus maintaining the gradient in the boundary layer.

**Table 8.** Streamline contours at AoA 15° for different inlet velocities (10–25 m/s) comparing cases without and with VG

| | AoA 15° | |
|---|---|---|
| 10 | 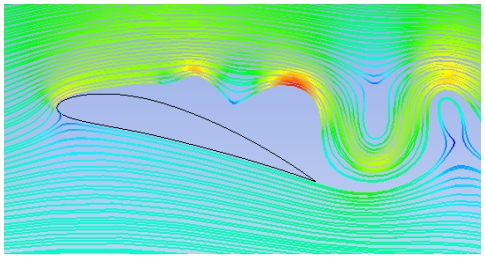 | 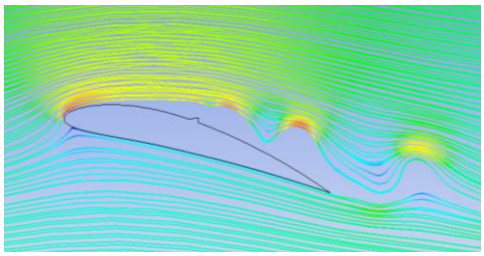 |
| 15 | 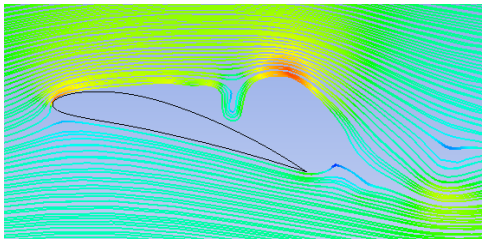 | 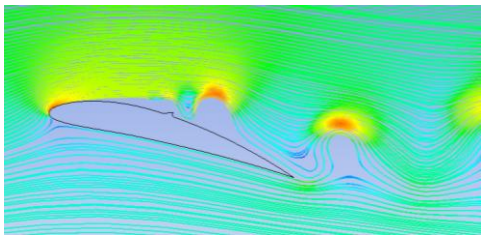 |
| 20 | 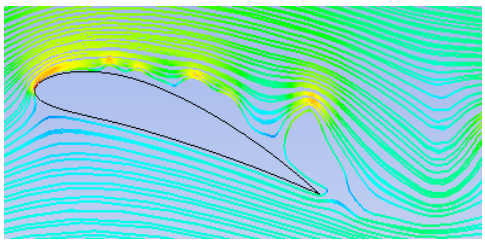 | 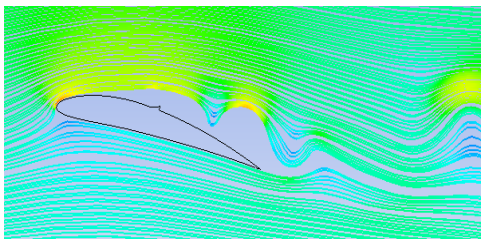 |
| 25 | 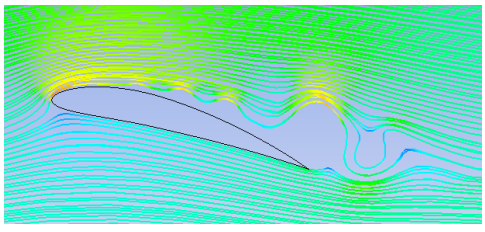 | 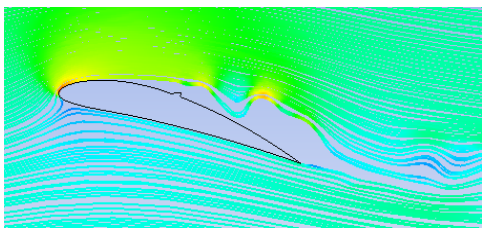 |

At high angles of attack, such as 15°, the airfoil has begun to enter a critical condition before stalling. Stall occurs when the airflow does not have enough momentum to continue to adhere to the airfoil, so that $C_L$ drops drastically and $C_D$ increases due to the influence of a large pressure gradient. The addition of a vortex generator delays the stall so that the airfoil still has lift at the critical angle of attack. At a velocity of 10 m/s, the $C_L$ value increases slightly by 5.49% with a large drag reduction of up to 44.37%. So the $C_L/C_D$ ratio increases significantly to 89.62%. This drastic increase indicates that at low velocities, the vortex generator plays a role in maintaining a stable airflow so that stall can be delayed. At a velocity of 15 m/s, the increase in the lift coefficient ($C_L$) is relatively

small, with an increase of only 1.34%. However, the drag coefficient ($C_D$) decreases drastically with a decrease of 44.73% so that the $C_L/C_D$ ratio experiences a significant increase to 83.02%. This confirms that the vortex generator improves aerodynamic performance at high angles of attack by reducing the drag coefficient so that the pressure gradient can be reduced. At a velocity of 20 m/s, the increase in $C_L$ compared to the previous velocity with an increase of 1.76%. While there was still a decrease in $C_D$ of 43.52%. This ratio resulted in $C_L/C_D$ being 80.16%. Slightly smaller than at the previous velocity because at the increased velocity, the momentum provided by kinetic energy is also greater. This increase in the lift coefficient was also seen to increase at a velocity of 25 m/s with an increase of 9.63%, the highest among all velocities tested. While $C_D$ decreased by 34.93% that the $C_L/C_D$ ratio increased by 68.49%. This increase appears to be the smallest compared to lower velocities, confirming that at high velocities, the momentum and kinetic energy are greater, so that the addition of a VG appears to experience a decrease in increasing airfoil efficiency.

The graphical representation (Figure 6(d)) also shows how the VG significantly improves aerodynamic performance, indicated by the large gap between the baseline airfoil and the VG airfoil at all velocities. This trend indicates that at high angles of attack, the VG is quite effective in redirecting the airflow (reattachment) that was previously separated from the beginning. In line with the streamlined visualization, it also shows a similar thing, where at the baseline airfoil, there is a large separation starting from 40% chord from the leading edge and extending to the trailing edge. Even at a velocity of 20 m/s, a fairly large reverse flow is seen on the trailing edge. With the addition of the VG, the airflow on the airfoil becomes more directed and more stable because the resulting vortex flow has greater momentum so that the wake area on the airfoil becomes smaller and more organized.

The aerodynamic performance of airfoils is highly sensitive to changes in the flow characteristics in the boundary layer. Previous studies [28] have shown that differences in geometry can significantly increase $C_L$ and $C_L/C_D$, which supports the results of this study, that the addition of VG affects the increase in $C_L/C_D$. Generally, the installed VG on NACA 6412 influenced the separation. As explained in the Results section, separation is suppressed, the flow remains more attached, and small vortices are observed that help delay stall. The VG produces streamwise vortices that inject kinetic energy into the boundary layer. This process stabilizes the flow at both low and high AoA, thereby reducing the wake behind the NACA 6412.

Although this research focused on the numerical analysis of the NACA 6412 airfoil with a VG, the findings also have broader practical implications. For example, the VG's ability to resist stall at moderate to high angles of attack could improve the maneuverability and safety of small UAVs, enhance the takeoff and landing performance of light aircraft, and improve the aerodynamic efficiency of wind turbine blades under varying wind conditions. These potential applications highlight the relevance of this research to real-world aerodynamic design.

## IV. Conclusions

The present study conducted numerical simulations using the Large Eddy Simulation (LES) method on the NACA 6412 airfoil with and without a vortex generator (VG). The addition of VG aimed to improve the aerodynamic performance by delaying the separation flow on the airfoil. This phenomenon is shown in Table 5, especially at AoA 10 and 15°.

The streamline exhibits the delay of the separation flow while VG was installed. It can be concluded that the use of VG has a significant impact on aerodynamic performance, especially at medium to high angles of attack. On the other hand, aerodynamic performance, which is indicated by the $C_L/C_D$ ratio, is also affected. At an angle of attack of 0°, the addition of VG does not provide a significant performance improvement and even tends to increase drag ($C_D$). Then, at an angle of attack of 5°, the $C_L/C_D$ ratio increases by approximately 5%, indicating the beginning of the VG's role in delaying flow separation. Furthermore, at an angle of attack of 10°, aerodynamic efficiency increases significantly, with the $C_L/C_D$ ratio increasing by 26% to 72%, depending on the flow velocity. At an angle of attack of 15°, the highest efficiency increase occurs, with the $C_L/C_D$ ratio increasing by 68% to 83%, indicating that the VG is highly effective in preventing stall. The effect of VG installation is most pronounced at low to medium velocities, as at high velocities, the free-stream energy is sufficient to maintain boundary layer stability without the aid of passive control devices.

This study has several limitations: the CFD approach provides a 2D solution, which is less accurate than a 3D one, and the airfoil only used one type of VG, so no comparative analysis could be performed. Future studies should extend the analysis into 3D approach to capture a more realistic contour and obtain more accurate aerodynamic data.

## Acknowledgment

The authors would like to express special gratitude to the Adisutjipto Institute of Aerospace Technology for the funding incentives for this research activity.

## References

[1] P.R. Krishnan, R. Mukesh, I. Hasan, P.B. Devi, and W.A. Alebachew, "Comparative Study and Aerodynamic Analysis of Rectangular Wing Using High-Lift Systems," *International Journal of Aerospace Engineering*, vol. 2023, 2023, doi: 10.1155/2023/5813557.

[2] F.E.C. Culick, and H.R. Jex, "Aerodynamics, Stability and Control of the 1903 Wright Flyer," in *AlAA Wright Flyer Project - Report WF84/09-1*, Smithsonian Institution; Dec. 16, 1983. Accessed: Sep. 16, 2025. [Online]. Available: https://www.researchgate.net/publication/48925494_Aerodynamics_Stability_and_Control_of_the_1903_Wright_Flyer

[3] A. Rizzi, "Separated and Vortical Flow in Aircraft Aerodynamics: A CFD Perspective," Jul. 15, 2023, *Cambridge University Press*. doi: 10.1017/aer.2023.39.

[4] S. Hariyadi and W.A. Widodo, "Efek Penggunaan Vortex Generator Terhadap Karakteristik Aliran pada Airfoil NACA 43018," *Jurnal Penelitian*, vol. 3, no. 4, pp. 62–70, 2018, doi: https://doi.org/10.46491/jp.v3i4.119.

[5] M. Özden, M.S. Genç, and K. Koca, "Passive Flow Control Application Using Single and Double Vortex Generator on S809 Wind Turbine Airfoil," *Energies (Basel)*, vol. 16, no. 14, Jul. 2023, doi: 10.3390/en16145339.

[6] S. N. Trysnavirensa, S. H. S. Putro, and N. Pambudiyatno, "The Effect of Triangular Vortex Generator Straight Arrangements on the NACA 0012 Airfoil Using A Smoke Generator," *Sainstech Nusantara*, vol. 2, no. 1, pp. 38–52, Feb. 2025, doi: 10.71225/jstn.v2i1.86.

[7] J.C. Lin, "Review of Research on Low-Profile Vortex Generators to Control Boundary-Layer Separation," *Progress in Aerospace Sciences*, vol. 38, pp. 389–420, 2002, doi: 10.1016/S0376-0421(02)00010-6.

[8] S. Arunvinthan, V.S. Raatan, S. Nadaraja Pillai, A.A. Pasha, M.M. Rahman, and K.A. Juhany, "Aerodynamic Characteristics of Shark Scale-Based Vortex Generators upon Symmetrical Airfoil," *Energies (Basel)*, vol. 14, no. 7, Apr. 2021, doi: 10.3390/en14071808.

[9] S. Hariyadi, W. Aries Widodo, B. Junipitoyo, and W. Suryono, "Studi Numerik dan Eksperimental Perbandingan Bentuk Vortex Generator dengan Posisi Straight pada Wing Airfoil NACA 43018," *Approach: Jurnal Teknologi Penerbangan*, vol. 2, no. 2, pp. 1–6, Oct. 2018, Accessed: Oct. 23, 2025. [Online]. Available: https://repo.poltekbangsby.ac.id/id/eprint/401

[10] T.S. Dharmawan, S. Hariyadi, and I.S. Rifdian, "Experimental Study of the Effect of Using A Gothic Vortex Generator Counter Rotating Arrangement on Wing Airfoil Eppler 562 with A Smoke Generator," in *Proceedings of the International Conference on Advance Transportation, Engineering, and Applied Science (ICATEAS 2022)*, Atlantis Press International BV, Feb. 2023, pp. 70–85. doi: 10.2991/978-94-6463-092-3_7.

[11] F. Kaya and H. Akbıyık, "Investigation of the Effects of Bioinspired Vortex Generators on Aerodynamic Performance of A NACA0015 Airfoil," *Bioinspiration & Biomimetics*, vol. 20, no. 1, Jan. 2025, doi: 10.1088/1748-3190/ada1bc.

[12] M. Seyhan, "Aerodynamic Characteristics and Flow Topology of Tapered Symmetrical Airfoil Equipped with Clark-Y Shaped Vortex Generators," *Physics of Fluids*, vol. 37, no. 1, Jan. 2025, doi: 10.1063/5.0249697.

[13] M. Algan, M. Seyhan, and M. Sarioğlu, "Effect of Aero-Shaped Vortex Generators on NACA 4415 Airfoil," *Ocean Engineering*, vol. 291, Jan. 2024, doi: 10.1016/j.oceaneng.2023.116482.

[14] X. Li, K. Yang, and X. Wang, "Experimental and Numerical Analysis of the Effect of Vortex Generator Height on Vortex Characteristics and Airfoil Aerodynamic Performance," *Energies (Basel)*, vol. 12, no. 5, Mar. 2019, doi: 10.3390/en12050959.

[15] Z. Zaheer, K.E. Reby Roy, G.S. Nair, V. Ragipathi, and U.V. Niranjan, "CFD Analysis of the Performance of Different Airfoils in Ground Effect," in *Journal of Physics: Conference Series*, Institute of Physics Publishing, Nov. 2019. doi: 10.1088/1742-6596/1355/1/012006.

[16] P. Gong, E. J. Aju, and Y. Jin, "On the Aerodynamic Loads and Flow Statistics of Airfoil with Deformable Vortex Generators," *Physics of Fluids*, vol. 34, no. 6, Jun. 2022, doi: 10.1063/5.0092187.

[17] G. Baldan and A. Guardone, "Wall-Resolved Large Eddy Simulations of A Pitching Airfoil in Deep Dynamic Stall," *Physics of Fluids*, vol. 37, no. 2, Feb. 2025, doi: 10.1063/5.0252828.

[18] W. Gao, W. Zhang, W. Cheng, and R. Samtaney, "Wall-Modelled Large-Eddy Simulation of Turbulent Flow Past Airfoils," *Journal of Fluid Mechanics*, vol. 873, pp. 174–210, Aug. 2019, doi: 10.1017/jfm.2019.360.

[19] A. Asnaghi, U. Svennberg, and R. E. Bensow, "Large Eddy Simulations of Cavitating Tip Vortex Flows," *Ocean Engineering*, vol. 195, Jan. 2020, doi: 10.1016/j.oceaneng.2019.106703.

[20] I. Ibarra-udaeta, K. Portal-Porras, A. Ballesteros-Coll, U. Fernandez-Gamiz, and J. Sancho, "Accuracy of the Cell-Set Model on A Single Vane-Type Vortex Generator in Negligible Streamwise Pressure Gradient Flow with RANS and LES," *Journal of Marine Science and Engineering*, vol. 8, no. 12, pp. 1–19, Dec. 2020, doi: 10.3390/jmse8120982.

[21] Z. Zhao, F. Wen, X. Tang, J. Song, Y. Luo, and Z. Wang, "Large Eddy Simulation of Film Cooling with Vortex Generators Between Two Consecutive Cooling Rows," *International Journal of Heat and Mass Transfer*, vol. 182, Jan. 2022, doi: 10.1016/j.ijheatmasstransfer.2021.121955.

[22] R. Stoll, J.A. Gibbs, S.T. Salesky, W. Anderson, and M. Calaf, "Large-Eddy Simulation of the Atmospheric Boundary Layer," *Boundary Layer Meteorology*, vol. 177, no. 2–3, pp. 541–581, Dec. 2020, doi: 10.1007/s10546-020-00556-3.

[23] R.K. Moghadam, K. Javadi, and F. Kiani, "Assessment of the LES-WALE and Zonal-DES Turbulence Models in Simulation of the Flow Structures Around the Finite Circular Cylinder," *Journal of Applied Fluid Mechanics*, vol. 9, no. 2, pp. 909–923, 2016, doi: 10.18869/acadpub.jafm.68.225.24280.

[24] M. Kim, J. Lim, S. Kim, S. Jee, and D. Park, "Assessment of the Wall-Adapting Local Eddy-Viscosity Model in Transitional Boundary Layer," *Computer Methods in Applied Mechanics and Engineering*, vol. 371, Nov. 2020, doi: 10.1016/j.cma.2020.113287.

[25] S. Koike, K. Nakakita, T. Nakajima, S. Koga, M. Sato, H. Kanda *et al.*, "Experimental Investigation of Vortex Generator Effect on Two- and Three-Dimensional NASA Common Research Models," in *53rd AIAA Aerospace Sciences Meeting*, American Institute of Aeronautics and Astronautics Inc, AIAA, 2015. doi: 10.2514/6.2015-1237.

[26] A. Seshagiri, E. Cooper, and L.W. Traub, "Effects of Vortex Generators on An Airfoil at Low Reynolds Numbers," *Journal of Aircraft*, vol. 46, no. 1, pp. 116–122, Jan. 2009, doi: 10.2514/1.36241.

[27] F. Huang, Z. Geng, B. Luo, Y. Peng, L. Xu, W. Wang *et al.*, "Simulation Analysis and Experimental Verification of High-Speed Impact of Rocky Asteroids," *Sensors*, vol. 25, no. 7, Apr. 2025, doi: 10.3390/s25072055.

[28] B.D. Susilo, G. Jatisukamto, and M.N. Kustanto, "Characteristic Analysis of Horizontal Axis Wind Turbine Using Airfoil NACA 4712," *Journal of Mechanical Engineering Science and Technology (JMEST)*, vol. 3, no. 2, pp. 96–108, Nov. 2019, doi: 10.17977/um016v3i22019p096.